Electronic correlation effects in reduced rutile TiO_2 within the LDA+U method

Seong-Geon Park,[1] Blanka Magyari-Köpe,[2] and Yoshio Nishi[2]
[1]*Department of Materials Science and Engineering, Stanford University, Stanford, California 94305, USA*
[2]*Department of Electrical Engineering, Stanford University, Stanford, California 94305, USA*
(Received 6 January 2010; revised manuscript received 30 July 2010; published 9 September 2010)

The structures and energies of oxygen-deficient rutile TiO_2 were calculated using density-functional theory. The electronic interactions are described within the LDA+U formalism, where on-site Coulomb corrections are applied on the 3d orbital electrons of Ti atoms (U^d) and 2p orbital electrons of the O atoms (U^p). We show that the U^d parameter affects only the character of the conduction band and values higher than 7 eV produce an unphysical description of the electronic interactions. The results are dramatically improved, when correlation corrections are introduced additionally on the O 2p orbitals by employing the LDA+U^d+U^p approach, and we observe systematic shifts for both the valence and conduction bands. This combined approach produces a corrected energy band structure and the band-gap energy is in very good agreement with experimental data. Using this approach for the oxygen-deficient structure, in the case of a neutral oxygen vacancy we find that the electrons from the Ti nearest to the vacancy become localized and induce defect states within the band gap, in very good agreement with experiment and other theoretical calculations. Additionally, these defect states are strongly limited on the three Ti atoms surrounding oxygen vacancy. The doubly positively charged oxygen vacancy is found to be more stable than neutral oxygen vacancy in most range of Fermi level and the vacancy-formation energies show significant dependence on the deposition conditions, i.e., Ti- or O-rich environments.

DOI: 10.1103/PhysRevB.82.115109 PACS number(s): 71.55.−i, 71.15.Mb

I. INTRODUCTION

Titanium dioxide, a material with a wide variety of applications, is used as photocatalyst, gas sensor, and semiconducting electrode in solar-cell devices. In addition, increased interest in the properties of TiO_2 emerged recently,[1] due to its "memristive" switching behavior in resistance random access memory applications, and it was proposed to be a strong candidate for the next generation of nonvolatile memories. The resistance switching behavior is controlled by the applied voltage or current pulse at the electrodes. Lattice defects in the bulk oxide or near the interface with the electrode are currently believed to play an important role in the switching between the resistive off state to a more conductive on state in this material. Based on experimental observations, several resistance-switching models have been suggested so far for transition-metal-oxide-based devices, such as charge trapping,[2] conductive filament formation,[3] Schottky barrier modulation,[4] and electrochemical migration of point defects.[5] However, the underlying principles of the switching mechanism are still lacking a detailed understanding, i.e., how to control and modulate the electrical characteristics of devices incorporating defects and impurities, such as oxygen vacancy, Ti interstitials, hydrogen, and other metallic atoms acting as dopants. In fact, several previous studies have shown that TiO_2 exhibits n-type semiconducting conductivity with extra electron carriers generated by the formation of oxygen vacancies.[6,7] Reduced TiO_2, in the phase diagram of the Ti-O system,[8] corresponds to several stable titanium-oxygen phases that exist between Ti_2O_3 and TiO_2, and therefore the oxygen vacancy can become the major point defect observed in TiO_2. The role of oxygen vacancies in TiO_2 has been extensively studied during the past decades by various experimental and theoretical methods; however, the effect of oxygen vacancy on the electronic band structure remains controversial. The experimental results of Cronemeyer[7] showed that two energy levels are generated by oxygen vacancy at 0.75 and 1.18 eV below the conduction-band minimum. However, Ghosh *et al.*[9] observed eight different energy levels within the band gap on the oxygen-deficient rutile TiO_2 sample. Theoretical study of Chen *et al.*[10] on reduced rutile TiO_2 showed that a defect state was produced 0.87 eV below the conduction-band minimum for neutral oxygen vacancy and 1.78 eV below the conduction-band minimum for positively charged oxygen vacancy. They employed an embedded-cluster numerical discrete variation method. Another investigation based on a semiempirical self-consistent method using the tight-binding model observed the oxygen-vacancy defect state at 0.7 eV below the conduction-band minimum. On the other hand, local-density approximation (LDA) calculation of Cho *et al.*[11] observed the oxygen-vacancy defect state above the conduction band. Another theoretical study of Ramamoorthy *et al.*[12] using *ab initio* self-consistent pseudopotential total-energy calculations found that oxygen vacancies introduce defect state at 0.3 eV below the conduction-band minimum. In this paper, we discuss the effect of electronic correlations on the energy band gap, atomic relaxation, charge density, and vacancy-formation energy of rutile TiO_2 by using density-functional theory and the LDA with the addition of on-site Coulomb corrections (LDA+U) method.[13]

In the past decade several theoretical investigations employed the local-density and the gradient corrected approximations to calculate the electronic structure of TiO_2.[14–16] Going beyond LDA, recent theoretical developments of exchange and correlation functionals, as the addition of the on-site Coulomb correction within LDA+U,[13] dynamical mean-field theory approaches,[17] the progress in hybrid functional,[18] and GW implementations[19] have been shown to

correct for some of the most severe shortcomings of the conventional LDA, i.e., the accurate prediction of the energy band gap and electronic defect states in transition-metal oxides.

Previous LDA+U studies,[20,21] however, did point to the fact that the energy band gap of rutile TiO_2 strongly depends on the U parameter, when the correction is applied on the Ti d orbitals and remains still underestimated compared to the experimental energy band gap of 3.0 eV, even at high values of U. A few earlier theoretical studies on transition-metal systems[22,23] discussed the effect of on-site Coulomb corrections on the p electrons (U^p) of the oxygen in addition to the d electrons (U^d) of the transition metal. According to Nekrasov *et al.*,[24] when self-interaction correction is implemented only to the d orbitals, the oxygen p orbitals do not shift from the LDA obtained positions and the occupied d band lies much lower than oxygen valence band. In order to improve this situation, self-interaction correction must be applied to all valence states including oxygen p orbitals. Therefore the correct description of the energy splitting between occupied and unoccupied orbitals can be obtained. Several theoretical studies has already reported about the effect of U^p values.[25–27] In the present study, we discuss the effect of U^p and U^d on the band structure of TiO_2 and show that the LDA+U method provides an improved band gap and position of the gap states if both U^d and U^p are used. We establish an upper limit U^d based on electronic structure of the conduction band, where unphysical overlap between the t_{2g} and e_g states is observed at values of U higher than 7 eV. Charged vacancy configurations had been investigated for the optimum U^d and U^p and a transition from the 2+ to 1+ and 1+ to neutral state is predicted at 0.7 eV and 0.1 eV, respectively, below the conduction band for the relaxed Ti-rich and O-rich samples.

II. COMPUTATIONAL METHODS

Density-functional calculations using the Vienna *ab initio* simulation package, (VASP) (Refs. 28–31) were carried out for the study of oxygen deficient rutile TiO_2. We used the LDA+U method for the description of the exchange and correlation energy of electrons. An energy cutoff of 353 eV was employed for the plane-wave expansion of electron wave functions. The ionic potentials are described by projector augmented-wave (PAW) pseudopotentials.[30] For k-point integration within the first Brillouin zone, $8\times8\times12$ Monkhorst-Pack grid for primitive cell and $4\times4\times4$ Monkhorst-Pack grid for supercell were selected. A pseudo-atomic calculation was performed for O $2s^2 2p^4$ and Ti $3s^2 3p^6 3d^2 4s^2$ states of valence electrons. All atoms were allowed to relax with energy convergence tolerance of 10^{-6} eV/atom and ground state was obtained by minimizing the force on each atom less than 0.001 eV/Å.

The oxygen vacancy was introduced within $2\times2\times3$ supercell of rutile TiO_2 so that it consists of 24 Ti and 47 O atoms. A larger supercell of $3\times3\times4$ with a total of 72 Ti and 143 O atoms was used to check for finite-size effects, and it was found that the vacancy-formation energy value changed only by 0.15 eV. On-site Coulomb correction between the p-orbital electrons of O (U^p) has been applied in addition to the correction for the d-orbital electrons in Ti (U^d). This approach will be referred to as LDA+U^d+U^p through this paper. In order to find the optimum U^d and U^p parameters, we applied various U^d and U^p ranging from 3 to 9 eV and investigated their effect on the band structure. For the exchange parameter J (Ref. 32) a value of 0.6 eV was used.

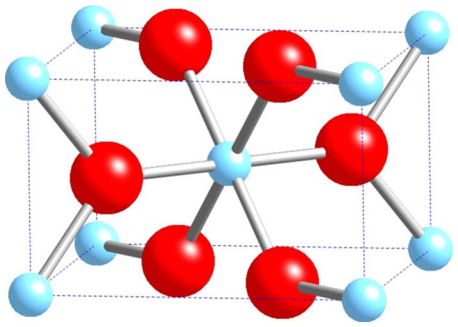

FIG. 1. (Color online) Unit-cell structure of rutile TiO_2. Small light blue ball denotes a Ti atom and big red one an O atom. Each Ti atom is surrounded by six O atoms.

III. RESULTS AND DISCUSSION

A. Bulk properties of rutile TiO_2

We first performed *ab initio* calculations for bulk rutile TiO_2. The unit-cell structure of rutile TiO_2 is illustrated in Fig. 1. Six O atoms, forming a distorted octahedral structure, surround the Ti atoms. Due to the different Ti-O bond lengths, Ti $3d$ orbitals will split into two sets of t_{2g} and e_g orbitals. e_g orbitals are associated with the upper conduction band and point at surrounding six oxygen atoms forming σ bonds. On the other hand, oxygen atoms are surrounded by three Ti atoms in a planar geometry. $2p$ orbitals of O atoms make three σ bonds with e_g orbitals of the surrounding Ti atoms. The partial density of Ti and O states of rutile TiO_2 for both LDA and GGA are shown in Fig. 2. The Fermi-level position is set to 0 eV. The valence-band states are mainly composed of O $2p$ hybridized with Ti $3d$ orbitals, and the top of the valence band is dominated by O $2p$ states. The

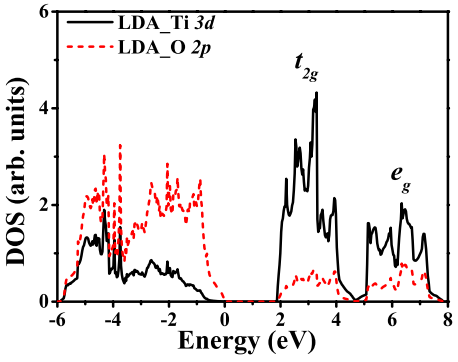

FIG. 2. (Color online) Partial density of states of Ti $3d$ orbital (solid line) and O $2p$ orbital (dotted line) calculated with LDA. The top of the valence band is set to the zero of energy.

TABLE I. Comparison of structural parameters a (Å) and c (Å), bulk modulus B (GPa), and band-gap energy E_g (eV) calculated by LDA+U^d with experimental results.

	U^d (eV)	a (Å)	c (Å)	c/a	B (GPa)	E_g (eV)
Expt. (Ref. 37)		4.584	2.953	0.644	284	3.00
GW (Ref. 38)		4.594	2.958	0.644		4.80
HSE (Ref. 39)		4.590	2.947	0.642		3.05
HSE (Ref. 40)		4.600	2.962	0.644	256	3.25
PW1PW (Ref. 41)		4.59	2.98	0.649	234	3.54
LDA (Ref. 11)		4.563	2.914	0.637	265	1.7
GGA		4.644	2.975	0.641	222	1.78
LDA		4.557	2.929	0.643	258	1.79
LDA+U^d	3	4.572	2.957	0.647	255	1.96
	4	4.579	2.969	0.648	254	2.04
	5	4.585	2.982	0.650	253	2.12
	6	4.591	2.994	0.652	252	2.21
	7	4.597	3.005	0.654	251	2.30
	8	4.603	3.016	0.655	250	2.40
	9	4.610	3.027	0.657	248	2.50

valence-band width of 6 eV is in good agreement with experimental measurements, which are in the range of 5–6 eV.[33,34] On the other hand, the conduction-band states have Ti 3d states with weak hybridization with O 2p states. The two peaks in the conduction band are a result of the ligand field splitting of the Ti 3d orbitals into two sets of t_{2g} and e_g states. We find no significant difference in the electronic structure obtained with LDA or GGA methods, both underestimate the band gap by about 44%.

There is no general consensus for LDA+U^d about how to find the optimum U^d value. Calzado *et al.*[20] suggested that a U^d_{eff} value ($U^d_{eff}=U^d-J$) of 5.5 ± 0.5 eV gives a correct description of the defect state using the LDA+U implementation in the VASP code. On the other hand, Deskins and Dupuis[35] chose a U^d_{eff} value of 10 eV using the same code which is found a band gap in satisfactory agreement with experiment for rutile TiO_2. In most LDA+U^d studies of transition-metal oxides, U^d values are fitted in an empirical way, but schemes based on theoretical determination of the U parameter had been also performed.[36] In order to investigate the effect of Coulomb correction for both Ti 3d orbital electrons and O 2p orbital electrons, we have employed several calculations, in which a range of U^d and U^p values were chosen. For validation, we have considered the structural parameters of rutile TiO_2, i.e., lattice constants and bulk modulus, the band-gap energy, the position of the defect state and vacancy-formation energy. Table I shows the structural parameters and band-gap energies calculated with increasing U^d value and in comparison with experimental results. Both lattice constants are found to increase with increasing U^d, however, the dependence of the bulk modulus on the U^d is negligible. The band-gap energy is increased with increasing U^d values from 3 to 9 eV, from a value of 1.79 eV obtained with the conventional LDA to 2.50 eV. This is in agreement

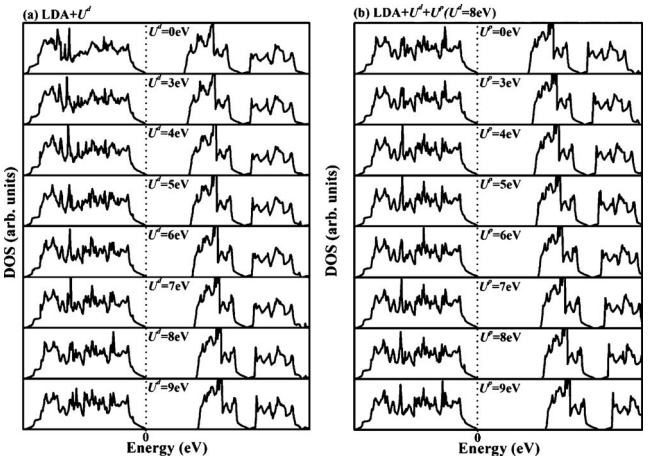

FIG. 3. The density of states obtained by (a) LDA+U^d and (b) LDA+U^d+U^p. The top of the valence band is set to the zero of energy. U^d and U^p range from 3 to 9 eV and U^d is fixed to 8 eV in the case of (b).

with previous theoretical investigations,[12] however, the band-gap energy is still underestimated compared to the experimental band-gap energy of 3.0 eV. This indicates that the LDA+U^d approach may not be adequate to calculate the electronic structure of rutile TiO_2. To improve on the on-site Coulomb corrections we propose to include additional corrections for the oxygen 2p orbitals (U^p). Figure 3(a) shows the density of states calculated by LDA+U^d, where U^d ranges from 3 to 9 eV and Fig. 3(b) corresponds to LDA+U^d+U^p calculations, where U^d is fixed to 8 eV and U^p ranges from 3 to 9 eV. The Fermi level is scaled to zero of energy. In order to more clearly show the difference among various U parameters, we have shown only the positive spin density of states although the density of states of TiO_2 had been calculated as a spin-polarized system.

For a better understanding of the effects of U^d and U^p, we evaluate the band structure calculated employing LDA+U^d and LDA+U^d+U^p, presented in Fig. 4. In the case of increasing U^d, while the conduction-band minimum is shifted upward, the valence band is not affected as shown in Fig.

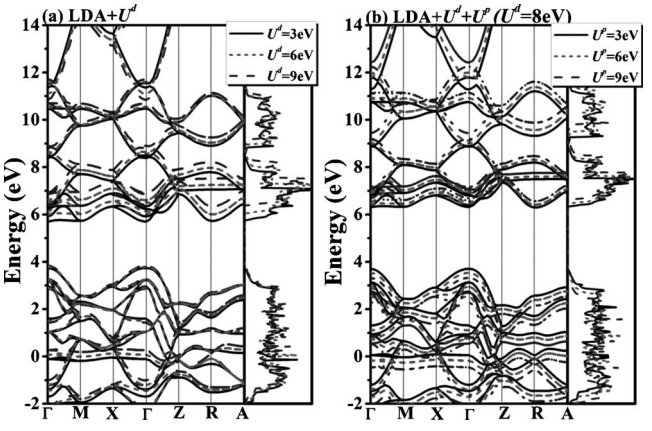

FIG. 4. The energy band structure and density of states calculated by (a) LDA+U^d and (b) LDA+U^d+U^p. Fermi level is not scaled at the zero of energy.

TABLE II. The structural parameters a (Å) and c (Å), bulk modulus B (GPa), and band-gap energy E_g (eV) calculated by LDA+U^d+U^p.

U^d (eV)	U^p (eV)	a (Å)	c (Å)	c/a	B (GPa)	E_g (eV)
8	3	4.574	3.004	0.657	290	2.58
8	4	4.562	2.997	0.657	282	2.67
8	5	4.547	2.993	0.658	289	2.77
8	6	4.532	2.986	0.659	269	2.87
8	7	4.518	2.980	0.660	269	2.98
8	8	4.500	2.973	0.661	281	3.11
8	9	4.483	2.965	0.661	296	3.24

4(a). However, calculations involving LDA+U^d+U^p show an upward shift of the conduction band as well as a downward shift of valence band, as shown in Fig. 4(b). The on-site Coulomb correction U^d+U^p increases the splitting between occupied and empty energy states, since the correction is dependent on the occupancy of the orbitals.[24] The energy states change character with U^d at several points, but, in particular, they are more severely affected at the Γ point. Figure 4(a) shows the band structure corresponding to U^d=3, 6, and 9 eV and in Fig. 4(b) U^d=8 eV is fixed while U^p=3, 6, and 9 eV.

It has been shown that rutile TiO_2 presents characteristics of a charge-transfer insulator.[11] Thus increased energy separation between Ti 3d and O 2p bands results in higher charge-transfer energy and ultimately leads to a more ionic character. The electronic population function corresponding to each individual atom was calculated using the Bader charge analysis. We find that by applying both U^d and U^p, the electron population on each Ti atom is reduced by 0.358e while that on each O atom is increased by 0.179e, indicating that the on-site Coulomb correction predicts a more ionic bonding character.

The calculated band gap is around 3.0 eV for U^d+U^p (8+6, 8+7, 8+8 eV) in good agreement with the experimental value.[37] The calculated structural parameters and band-gap energies for several combinations of U^d and U^p are shown in Table II. We find that the correction on the energy band gap due to U^p is comparable to that due to U^d, indicating that the adequate description of the on-site Coulomb interactions of the p-orbital electrons of O atom is as significant as is for the metal d-orbital electrons, a feature also observed by Nekrasov *et al.*[24] for other transition-metal oxides.

B. Oxygen vacancy in TiO_2

It is well known that the oxygen vacancies play an important role in the electrical conductivity of TiO_2. We first employed LDA+U^d method in the calculation of electronic structure of 2×2×3 TiO_2 supercell incorporating one oxygen vacancy. Total density of states for several values of U^d ranging from 3 to 9 eV is shown in Fig. 5(a). The conventional LDA yields no defect state in the band gap (not shown). As U^d value increases, the conduction bands shift toward higher energy states, and thus the defect state is separated from conduction band for U^d values larger than 5 eV. The distance between the localized defect state and the top of the valence bands is constant, regardless of the U^d value. With the removal of an oxygen atom a neutral oxygen vacancy is created, two electrons that previously occupied oxygen 2p orbitals become localized. These electrons may be responsible for the n-type transport behavior[6,7] depending on the position of the defect states in the band gap. Therefore, the correct prediction of the defect state has important implications for applications and methods beyond LDA are necessary to employ. We find that the defect states generated by oxygen vacancy shows mainly Ti 3d character and minor O 2p, indicating a high localization of the two electrons from the three nearest-neighboring Ti atoms surrounding the oxygen vacancy. Pointing to the limitation of using large U^d, an additional defect state in the band gap is observed for U^d =8 and 9 eV. We find that this defect state is an artifact caused by the large U^d, its origin is unphysical and different from that of the previous defect state. The effect of the increasing U^p is shown in Fig. 5(b), the valence band is gradually shifted downward, and the position of the defect state is not affected.

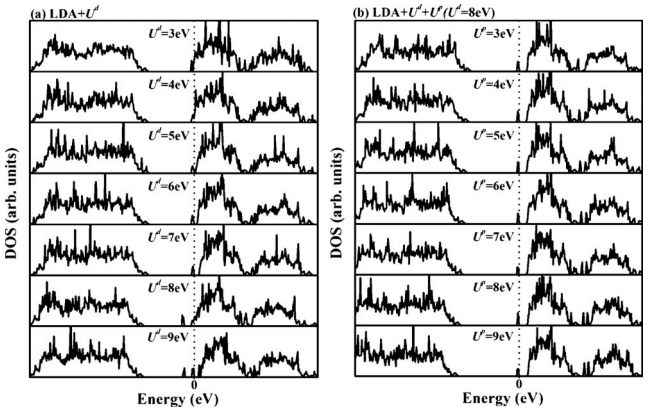

FIG. 5. The density of states of 2×2×3 supercell TiO_2 with oxygen vacancy calculated by (a) LDA+U^d and (b) LDA+U^d+U^p. U^d and U^p ranges from 3 to 9 eV and U^d is fixed to 8 eV in the case of (b). Spin-down density of states is not shown.

In rutile TiO_2, due to the different bond lengths, the three Ti atoms surrounding the oxygen vacancy are grouped as two atoms of type-I Ti and one atom of type-II Ti. These Ti atoms and oxygen vacancy are in the same plane (110). The partial densities of states of the Ti atoms surrounding the oxygen vacancy are displayed in Fig. 6, calculated for U^d=7 and 8 eV. There is only one defect state on type-II Ti atoms for $U^d \leq 7$ eV, indicating that the two electrons which are left behind by the removed oxygen are strongly localized on the 3d orbitals of the three Ti atoms. These two electrons are occupied by a spin-up and spin-down defect states which are localized at the same energy level. (The spin-down density of states is not shown.) Then, an additional defect state of small intensity on type-II Ti atom is observed for U^d is 8 eV. We confirmed that spin-up and -down defect states are observed at the same energy level up to U^d=7 eV. Several previous theoretical studies have reported that oxygen vacancy gives

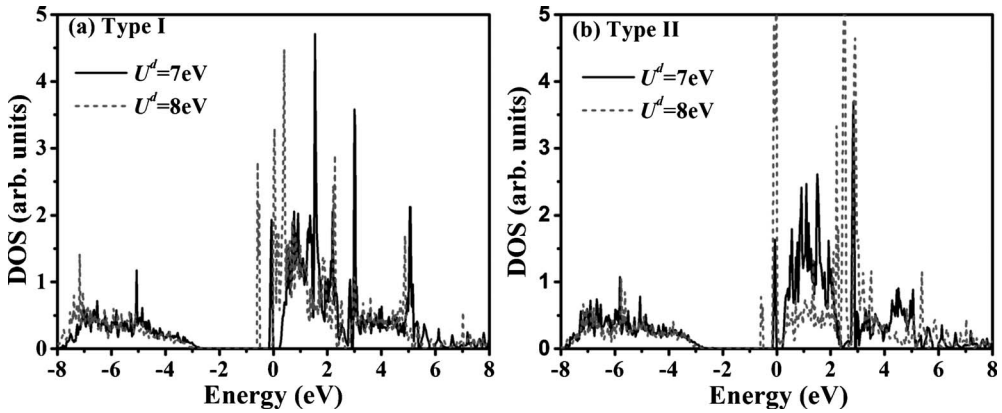

FIG. 6. Partial density of states of three neighboring Ti atoms surrounding oxygen vacancy calculated by LDA+U^d (U^d=7 and 8 eV). (a) Type-I Ti and (b) type-II Ti. Additional defect state is observed for U^d=8 eV.

rise to one energy level of defect states in TiO_2.[10–12] For U^d=8 eV, however, the spin-down defect state disappears and two spin-up defect states at a different energy level are observed as shown in Fig. 6. This is clearly an artifact observed at large U^d, supported also by the altering character of the partial conduction-band structure. We also observed similar changes in density of states for U^d of 9 eV. Therefore, an excess of Coulomb correction on the d orbitals may cause local distortion in the electronic structure, and therefore its usage should be well tested.

In order to understand the physical effects of how U^d affects the atomic bonding in TiO_2, the valence charge electron localization functions (ELF) were calculated by using this formula:[42]

$$\mathrm{ELF} = (1 + \chi_\sigma^2)^{-1}, \tag{1}$$

where

$$\chi_\sigma = \frac{D_\sigma}{D_\sigma^0} \tag{2}$$

and

$$D_\sigma^0 = \frac{3}{5}(6\pi^2)^{2/3}\rho_\sigma^{5/3}, \tag{3}$$

where ρ is the electron spin density and D_σ^0 corresponds to a uniform electron gas with spin density equal to the local value of $\rho_\sigma(r)$. The ratio χ_σ is thus a dimensionless localization index calibrated with respect to the uniform density electron gas as reference. ELF gives account of the type of bonding preferred and has a value between 0 and 1. The value of 1 corresponds to perfectly localized regions, showing mostly covalent bonding character. 0.5 corresponds to electron gas indicating metallic nature while values between 0 and 0.5 indicate regions of low electron density, where strong ionic interactions are dominated. The ELF for U^d=7 and 8 eV is shown in Fig. 7. The red region (core region of each atom) in the oxygen-vacancy site shows that two electrons are highly localized on the 3d orbitals in the proximity of the vacancy site. The key difference of ELF between LDA+U^d of 7 eV and LDA+U^d of 8 eV is the bonding character for the nearest-neighboring Ti atoms and oxygen vacancy. Electronic charge is transferred to the oxygen vacancy from the type-II Ti atom. The electron density increases between the type-I Ti atoms and oxygen vacancy for U^d=8 eV as compared to U^d=7 eV, showing enhanced hybridization between type-I Ti and vacancy site with increasing U^d and increased Coulomb repulsion between type-II Ti

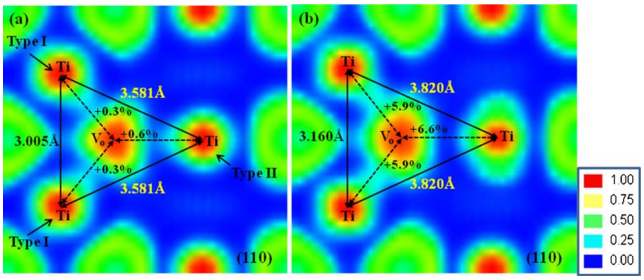

FIG. 7. (Color online) ELF and corresponding structural relaxation around neutral oxygen vacancy calculated by (a) LDA+U^d (U^d=7 eV) and (b) LDA+U^d (U^d=8 eV). Electrons are hardly found in the blue region (background, ELF 0) and electrons are highly localized in the red region (core region of each atom, ELF 1).

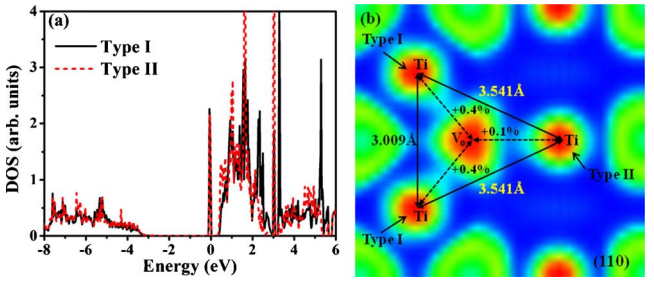

FIG. 8. (Color online) (a) Partial density of states of Ti atoms surrounding oxygen vacancy calculated by LDA+U^d+U^p (U^d=8 eV and U^p=6 eV). (b) Electron localization function and structural relaxations of rutile TiO_2 with one oxygen vacancy calculated by LDA+U^d+U^p (U^d=8 eV and U^p=6 eV).

TABLE III. Theoretical results of oxygen-vacancy-formation energy in rutile TiO_2.

Method	Code	Potential	E_{vf} (eV)	Reference
GGA	CRYSTAL03		4.47	Islam *et al.* (Ref. 41)
PW1PW	CRYSTAL03		5.08	Islam *et al.* (Ref. 41)
LDA	VASP	PAW	4.44	Cho *et al.* (Ref. 11)
GGA	VASP	U.S.-PP	4.52	Bouzoubaa *et al.* (Ref. 43)
LDA	QUANTUM-ESPRESSO	U.S.-PP	6.03	Hameeuw *et al.* (Ref. 44)
GGA	VASP	PAW	5.10	Shu *et al.* (Ref. 45)
GGA	VASP	U.S.-PP	4.93	Iddir *et al.* (Ref. 46)
HSE	VASP	PAW	5.50	Janotti *et al.* (Ref. 39)
LDA	VASP	PAW	4.61	This work

and the vacancy site. This significant change in the bonding character is strongly related to the atomic relaxation around the vacancy. The atomic displacements are the measured distances of the relaxed Ti atoms relative to the oxygen-vacancy site. After relaxation, the three Ti atoms surrounding the oxygen vacancy show outward relaxation from the vacancy while the oxygen atoms show inward relaxation. This relaxation trend in TiO_2 is controlled by the amount of charge transfer from the Ti ions, as has been also observed in other studies.[41] However, there is a great discrepancy between the amount of displacement of type-I and type-II Ti atoms for LDA+U^d with U^d=7 and 8 eV. For U^d=7 eV the type-I and type-II Ti atoms move away from vacancy by 0.3% and 0.6%, respectively. Nevertheless, the U^d=8 eV calculation shows that type-I and type-II Ti atoms are relaxed by 5.9% and 6.6%, respectively, significantly larger than the atomic displacement for U^d=7 eV. This fact suggests that there are indeed serious limitations for increasing U^d above 7 eV. It is interesting to note that this additional defect state, the distorted conduction bands and the enhanced relaxation observed for strong U^d (8 and 9 eV) disappear if U^p is employed in addition, at larger U^d values, in the LDA+U calculation. The partial density of states of type-I and type-II Ti atoms and ELF for LDA+U^d+U^p (U^d=8 eV and U^p=6 eV) are shown in Fig. 8, where density of states exhibits neither additional band-gap states nor distorted conduction bands as well as ELF shows similar bonding character with LDA+U^d (U^d=7 eV). These results lead us to the conclusion that the over correction caused by the strong U^d can be compensated by U^p, and thus yielding a much better agreement with experiment on the structural and electronic parameters of rutile TiO_2.

Next, we turn to the calculation of the oxygen-vacancy-formation energy. The formation energy of neutral oxygen vacancy E_{vf} (eV) is calculated as

$$E_{vf} = E(V_O) - E(TiO_2) + \mu_O, \quad (4)$$

where $E(V_O)$ is the total energy of the TiO_2 supercell containing one neutral oxygen vacancy and $E(TiO_2)$ is the total energy of the perfect TiO_2 crystal in the same supercell. μ_O is an oxygen chemical potential. With pure LDA, the calculated total energy of oxygen molecule is −10.66 eV. Assuming μ_O is half the total energy of an oxygen molecule, the formation energy is 4.61 eV. There have been few theoretical attempts to calculate the formation energy of oxygen vacancy and the values obtained along with the approximations used are shown in Table III. Islam *et al.*[41] calculated the formation energy of oxygen vacancy to be 4.47 eV with the GGA which agrees well with the value of 4.44 obtained by Cho *et al.*[11] obtained with LDA. Bouzoubaa *et al.*[43] also reported that the formation energy of oxygen vacancy is 4.52 eV with GGA. In contrast, using LDA, Hameeuw *et al.*[44] obtained the formation energy of oxygen vacancy of 6.03 eV. Shu *et al.*[45] and Iddir *et al.*[46] found that the GGA bulk vacancy-formation energies are 5.1 eV and 4.93 eV, respectively. Therefore, there is considerable controversy about the calculation of the formation energy of the oxygen vacancy in TiO_2. Experimental results of Kofstad[47] and Marucco *et al.*[48] showed that the formation enthalpy of doubly ionized oxygen vacancy is 4.55 eV and 4.57 eV, respectively. Additionally Marucco *et al.* observed that full ionization energies of neutral oxygen vacancy are not greater than 0.30 eV. Therefore the experimental formation energy of neutral oxygen vacancy should be less than 4.55 eV by the amount of 0.3 eV. The formation energies of oxygen vacancy obtained from the LDA+U calculations for various U^d and U^p values are presented in Table IV. U^p corrections are included in the calculation of the energy of oxygen molecule. The formation energies with LDA+U calculations are slightly larger than that with the conventional pure LDA. Although there are small discrepancies in vacancy-formation energies, these values are almost independent of U parameters, since Eq. (1) includes the reference energy for the oxygen molecule, which is corrected by U^p parameters, and the U^d and U^p corrections are applied the total energy of TiO_2 supercell. It is worth noting that absolute values of the for-

TABLE IV. The formation energy of oxygen vacancy with various values of U^d and U^p.

U^d (eV)	3	4	5	6	7	8	9
E_{vf} (eV)	5.41	5.68	6.05	6.10	6.11	5.83	5.66
U^p (U^d=8 eV)	3	4	5	6	7	8	9
E_{vf} (eV)	6.21	6.26	6.31	6.37	6.43	6.50	6.58

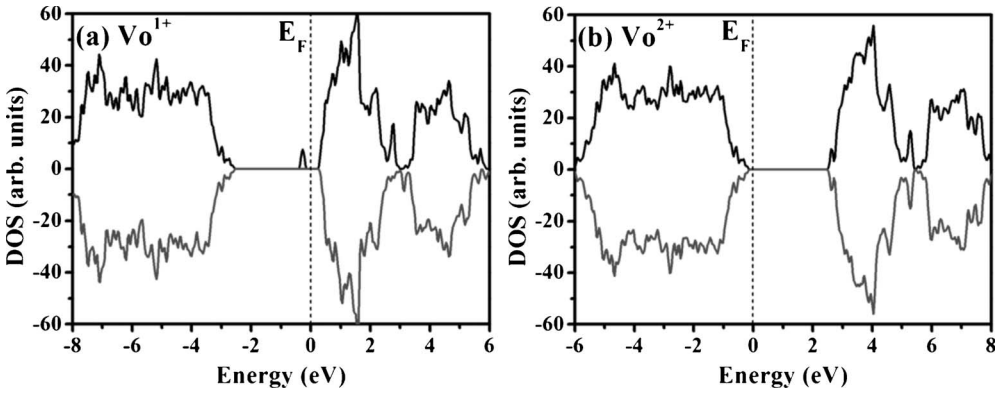

FIG. 9. Total spin density of states of rutile TiO_2 with (a) V_O^{1+} and (b) V_O^{2+} calculated by LDA+U^d+U^p (U^d=8 eV and U^p=6 eV).

mation energies calculated with the LDA+U method, as a function of U, are arbitrarily determined. Therefore, it is more practical to examine the transition states between different charged states of the vacancies then the absolute values of the formation energies.

In real TiO_2, it is well known that positively charged oxygen vacancies effectively dope TiO_2 with electrons, resulting in n-type semiconducting behavior.[49] As shown in Fig. 9, we calculated the spin density of states of rutile TiO_2 with positively charged oxygen vacancies. LDA+U^d+U^p, where U^d =8 eV and U^p=6 eV, is used in this calculation. In the case of singly charged oxygen vacancy (V_O^{1+}), the spin-down defect state shift toward the conduction-band minimum whereas both spin-up and -down defect states are observed below the conduction minimum for doubly charged oxygen vacancy (V_O^{2+}). This asymmetric density of states particularly in V_O^{1+} results in the ferromagnetic effect of undoped rutile TiO_2. Several experiments and theoretical investigations reported that the oxygen vacancy induces a magnetic moment in rutile TiO_2.[50,51] The different behavior of the electronic states in different charge state of the oxygen vacancy is linked to the atomic displacement of nearest-neighboring atoms surrounding oxygen vacancy. Figure 10 shows ELF and structural relaxations of TiO_2 with charged oxygen vacancy. The neighboring Ti atoms show outward relaxation 5.8–7.6 % for V_O^{1+} and 12% for V_O^{2+}, respectively, which are much larger relaxation than 0.4% outward relaxation in neutral oxygen vacancy. Similar results were observed by Janotti and Van de Walle for ZnO.[52] With the removal of electrons

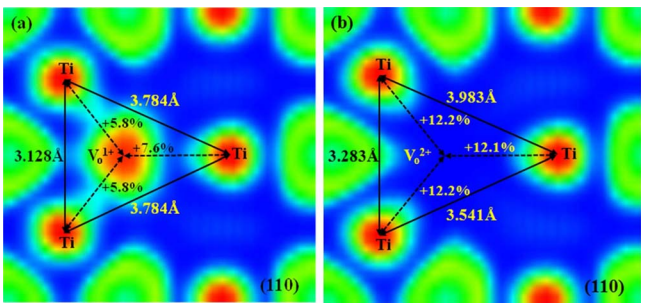

FIG. 10. (Color online) Electron localization function and structural relaxations around charged oxygen vacancy in LDA+U^d+U^p (U^d=8 eV and U^p=6 eV). (a) V_O^{1+} and (b) V_O^{2+}.

from oxygen vacancies a weaker Coulomb interaction between Ti atoms and the vacancy site is observed, resulting in larger displacement of the neighboring Ti atoms. As a result, the empty defect states shift toward the bottom of the conduction band.

To determine the relative stability of the various charge states of oxygen vacancy, we calculated the vacancy-formation energy of the positively and negatively charged oxygen vacancies using the following formula:

$$E_{vf}(V^q) = E(V^q) - E(TiO_2) + 1/2E(O_2) + \mu_O + qE_F, \quad (5)$$

(Ref. 39) where $E(V^q)$ is the total energy of the supercell containing a vacancy in charge state q and $E(TiO_2)$ is the total energy of perfect supercell. μ_O is the chemical potential of oxygen atom, which is a variable. This chemical potential must satisfy the growth condition of TiO_2, namely, μ_{Ti} +2μ_O=$\Delta H_f^{TiO_2}$=−11.1 eV. In the extreme O-rich limit, μ_O =0. The Ti-rich limit is constrained by the formation of Ti_2O_3; $2\mu_{Ti}+3\mu_O \leq \Delta H_f^{Ti_2O_3}$=19.1 eV, which gives μ_O =3.17 eV. The Fermi level E_F is referenced to the valence-band maximum (E_F=0 eV) and E_F term includes the energy of the valence-band maximum in the stoichiometric system and core-level electrostatic potential alignment between the defect supercell and the perfect crystal. The calculated vacancy-formation energies in relaxed and unrelaxed TiO_2 supercells as a function of Fermi level are shown in Figs. 11(a) and 11(b). Structural relaxation lowers the formation energy of neutral vacancy (V_O) and singly charged vacancy (V_O^{1+}) by amount of 0.23 eV and 1.28 eV, respectively. For the doubly charged vacancy (V_O^{2+}), relaxation lowers the formation energy by 2.95 eV, which is consistent with the different amount of lattice relaxation with respect to the charge state as described above. We find the transition levels $\varepsilon(2+/+)$ and $\varepsilon(1+/0)$ to be located in the band gap around 0.7 eV and 0.1 eV, respectively, below the conduction-band minimum. The lowest formation energy of the doubly charged vacancy (V_O^{2+}) for a wide range of Fermi level accounts for the observed n-type semiconducting behavior in TiO_2. Janotti *et al.*[39] have been studied the vacancy-formation energy in rutile TiO_2 using hybrid functional approximations (HSE). Similar behavior of lattice relaxation was found for the various charge states of oxygen vacancy. According to Janotti's work, V_O^{2+} has the lowest formation

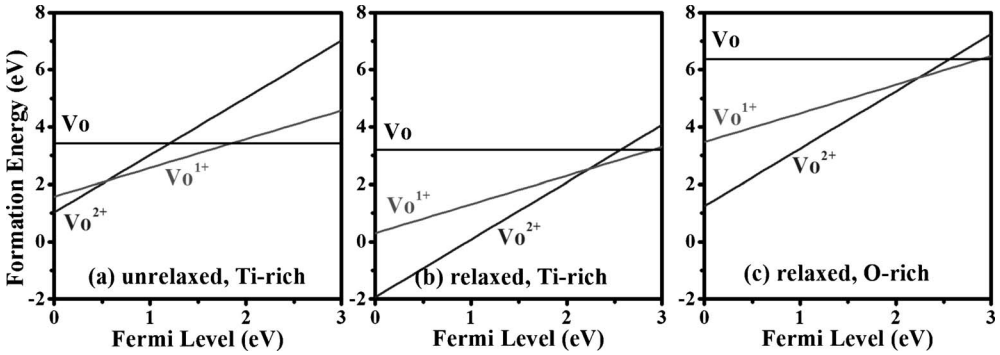

FIG. 11. The oxygen-vacancy-formation energy in rutile TiO_2 as a function of Fermi level. (a) unrelaxed in Ti-rich condition, (b) relaxed in Ti-rich condition, and (c) relaxed in O-rich condition.

energy for all values of the Fermi level and the transition levels $\varepsilon(2+/+)$ and $\varepsilon(1+/0)$ are located above the conduction-band minimum. This difference is attributed to the electronic correlation approximations and remains to be elucidated further for the LDA+U and HSE approximations. Although there is a small difference, our results for the formation of the charged vacancies essentially agree with the results in several previous studies.[46,53,54] The vacancy-formation energy of rutile TiO_2 in the limit of Ti-rich and O-rich are shown in Figs. 11(b) and 11(c). The formation energy of the various charge states of the vacancy in Ti-rich condition is lower than that in O-rich condition. The oxygen-vacancy concentration increases when the chemical potential of oxygen is lowered, due to its lower formation energy in Ti-rich (O-poor) condition. Several experimental studies[55,56] observed that electrical conductivity of TiO_2 was found to decrease with increasing oxygen partial pressure, i.e., the oxygen-vacancy concentration might be crucial for fine tuning the electrical properties of rutile TiO_2.

IV. CONCLUSION

In summary, we have performed LDA calculation corrected by including on-site Coulomb corrections between 3d orbital electrons of Ti atoms and 2p orbital electrons of O atoms for the study of oxygen-deficient rutile TiO_2. The obtained band-gap energy obtained by this calculation method is in very good agreement with experimental value. The addition of Coulomb corrections for 2p orbital electrons (U^p) provides an improved description of the electronic properties. We find that the defect states associated with the oxygen vacancy are positioned band gap. The electrons occupying the defect state are localized on the 3d orbitals of the three Ti atoms surrounding the oxygen vacancy. The formation energy of the doubly positively charged oxygen vacancy is the lowest for a wide range of Fermi level values, in agreement with the largest lattice relaxations around doubly charged oxygen vacancy. The formation energy of oxygen vacancy is a variable, which is strongly affected by the vacancy concentration in the sample. Compared to the O-rich limit condition, the formation energy in Ti-rich (O-poor) limit condition is lowered by 3.18 eV, indicating that higher oxygen-vacancy concentration leads to an improved conduction in rutile TiO_2.

ACKNOWLEDGMENTS

This work was supported by Stanford NMTRI project and MSD in Marco Focus Center. The computational work was carried out through the National Nanotechnology Infrastructure Network's Computational cluster at Stanford and Harvard University.

[1] J. J. Yang, M. D. Pickett, X. Li, D. A. A. Ohlberg, D. R. Stewart, and R. S. Williams, Nat. Nanotechnol. **3**, 429 (2008).
[2] A. Chen, S. Haddad, Y. C. Wu, Z. Lan, T. N. Fang, and S. Kaza, Appl. Phys. Lett. **91**, 123517 (2007).
[3] D. C. Kim, S. Seo, S. E. Ahn, D. S. Suh, M. J. Lee, B. H. Park, I. K. Yoo, I. G. Baek, H. J. Kim, E. K. Yim, J. E. Lee, S. O. Park, H. S. Kim, U.-In. Chung, J. T. Moon, and B. I. Ryu, Appl. Phys. Lett. **88**, 202102 (2006).
[4] T. Fujii, M. Kawasaki, A. Sawa, H. Akoh, Y. Kawazoe, and Y. Tokura, Appl. Phys. Lett. **86**, 012107 (2004).
[5] X. Guo, C. Schindler, S. Menzel, and R. Waser, Appl. Phys. Lett. **91**, 133513 (2007).
[6] M. D. Earle, Phys. Rev. **61**, 56 (1942).
[7] D. C. Cronemeyer, Phys. Rev. **113**, 1222 (1959).
[8] G. V. Samsonov, *The Oxide Handbook* (IFI/Plenum Press, New York, 1982).
[9] A. K. Ghosh, F. G. Wakim, and R. R. Addiss, Jr., Phys. Rev. **184**, 979 (1969).
[10] J. Chen, L.-B. Lin, and F.-Q. Jing, J. Phys. Chem. Solids **62**, 1257 (2001).
[11] E. Cho, S. Han, H.-S. Ahn, K.-R. Lee, S. K. Kim, and C. S. Hwang, Phys. Rev. B **73**, 193202 (2006).
[12] M. Ramamoorthy, R. D. King-Smith, and D. Vanderbilt, Phys. Rev. B **49**, 7709 (1994).
[13] S. L. Dudarev, G. A. Botton, S. Y. Savrasov, C. J. Humphreys, and A. P. Sutton, Phys. Rev. B **57**, 1505 (1998).
[14] S. B. Sinnott, R. F. Wood, and S. J. Pennycook, Phys. Rev. B **61**, 15645 (2000).

[15] K. M. Glassford and J. R. Chelikowsky, Phys. Rev. B **46**, 1284 (1992).
[16] C. Lee, P. Ghosez, and X. Gonze, Phys. Rev. B **50**, 13379 (1994).
[17] A. I. Liechtenstein, V. I. Anisimov, and J. Zaanen, Phys. Rev. B **52**, R5467 (1995).
[18] J. Heyd, G. E. Scuseria, and M. Ernzerhof, J. Chem. Phys. **118**, 8207 (2003).
[19] S. V. Faleev, M. van Schilfgaarde, and T. Kotani, Phys. Rev. Lett. **93**, 126406 (2004).
[20] C. J. Calzado, N. C. Hernandez, and Javier Fdez. Sanz, Phys. Rev. B **77**, 045118 (2008).
[21] A. Rubio-Ponce, A. Conde-Gallardo, and D. Olguin, Phys. Rev. B **78**, 035107 (2008).
[22] A. K. McMahan, R. M. Martin, and S. Satpathy, Phys. Rev. B **38**, 6650 (1988).
[23] M. S. Hybertsen, M. Schluter, and N. E. Christensen, Phys. Rev. B **39**, 9028 (1989).
[24] I. A. Nekrasov, M. A. Korotin, and V. I. Anisimov, e-print arXiv:cond-mat/0009107v1 (unpublished).
[25] B. J. Morgan and G. W. Watson, Phys. Rev. B **80**, 233102 (2009).
[26] M. Nolan and G. W. Watson, J. Chem. Phys. **125**, 144701 (2006).
[27] S. Lany and A. Zunger, Phys. Rev. B **80**, 085202 (2009).
[28] G. Kresse and J. Furthmüller, Phys. Rev. B **54**, 11169 (1996).
[29] G. Kresse and J. Furthmüller, Comput. Mater. Sci. **6**, 15 (1996).
[30] P. E. Blöchl, Phys. Rev. B **50**, 17953 (1994).
[31] G. Kresse and D. Joubert, Phys. Rev. B **59**, 1758 (1999).
[32] E. Pavarini, S. Biermann, A. Poteryaev, A. I. Lichtenstein, A. Georges, and O. K. Andersen, Phys. Rev. Lett. **92**, 176403 (2004).
[33] J. C. Woicik, E. J. Nelson, L. Kronik, M. Jain, J. R. Chelikowsky, D. Heskett, L. E. Berman, and G. S. Herman, Phys. Rev. Lett. **89**, 077401 (2002).
[34] L. D. Finkelstein, E. Z. Kurmaev, M. A. Korotin, A. Moewes, B. Schneider, S. M. Butorin, J.-H. Guo, J. Nordgren, D. Hartmann, M. Neumann, and D. L. Ederer, Phys. Rev. B **60**, 2212 (1999).
[35] N. A. Deskins and M. Dupuis, Phys. Rev. B **75**, 195212 (2007).
[36] A. Janotti, D. Segev, and C. G. Van de Walle, Phys. Rev. B **74**, 045202 (2006).
[37] U. Diebold, Surf. Sci. Rep. **48**, 53 (2003).
[38] M. Oshikiri, M. Boero, J. Ye, F. Aryasetiawan, and G. Kido, Thin Solid Films **445**, 168 (2003).
[39] A. Janotti, J. B. Varley, P. Rinke, N. Umezawa, G. Kresse, and C. G. Van de Walle, Phys. Rev. B **81**, 085212 (2010).
[40] H. Nakai, J. Heyd, and G. E. Scuseria, J. Comput. Chem. **5**, 7 (2006).
[41] M. M. Islam, T. Bredow, and A. Gerson, Phys. Rev. B **76**, 045217 (2007).
[42] A. D. Becke and K. E. Edgecombe, J. Chem. Phys. **92**, 5397 (1990).
[43] A. Bouzoubaa, A. Markovits, M. Calatayud, and C. Minot, Surf. Sci. **583**, 107 (2005).
[44] K. Hameeuw, G. Cantele, D. Ninno, F. Trani, and G. Iadonisi, Phys. Status Solidi A **203**, 2219 (2006).
[45] D.-J. Shu, S.-T. Ge, M. Wang, and N.-B. Ming, Phys. Rev. Lett. **101**, 116102 (2008).
[46] H. Iddir, S. Öğüt, P. Zapol, and N. D. Browning, Phys. Rev. B **75**, 073203 (2007).
[47] P. Kofstad, *Nonstoichometry, Diffusion, and Electrical Conductivity in Binary Metal Oxides* (Wiley, New York, 1972), Chap. 8.
[48] J. F. Marucco, J. Gautron, and P. Lemasson, J. Phys. Chem. Solids **42**, 363 (1981).
[49] E. G. Eror, J. Solid State Chem. **38**, 281 (1981).
[50] D. Kim, J. Hong, Y. Park, and K. Kim, J. Phys.: Condens. Matter **21**, 195405 (2009).
[51] N. H. Hong, J. Sakai, N. Poirot, and V. Brizé, Phys. Rev. B **73**, 132404 (2006).
[52] A. Janotti and C. G. Van de Walle, Appl. Phys. Lett. **87**, 122102 (2005).
[53] J. M. Sullivan and S. C. Erwin, Phys. Rev. B **67**, 144415 (2003).
[54] S. Na-Phattalung, M. F. Smith, K. Kim, M.-H. Du, S.-H. Wei, S. B. Zhang, and S. Limpijumnong, Phys. Rev. B **73**, 125205 (2006).
[55] R. K. Sharma, M. C. Bhatnagar, and G. L. Sharma, Appl. Surf. Sci. **92**, 647 (1996).
[56] J. Yahia, Phys. Rev. **130**, 1711 (1963).